THE JOURNAL OF BIOLOGICAL CHEMISTRY
Vol. 276, No. 17, Issue of April 27, pp. 14067–14074, 2001

*Printed in U.S.A.*

# Structure of Tctex-1 and Its Interaction with Cytoplasmic Dynein Intermediate Chain*

Received for publication, December 18, 2000, and in revised form, January 5, 2001
Published, JBC Papers in Press, January 8, 2001, DOI 10.1074/jbc.M011358200

**Yu-Keung Mok, Kevin W.-H. Lo, and Mingjie Zhang‡**

*From the Department of Biochemistry, the Hong Kong University of Science and Technology, Clear Water Bay, Kowloon, Hong Kong, People's Republic of China*

**The minus-ended microtubule motor cytoplasmic dynein contains a number of low molecular weight light chains including the 14-kDa Tctex-1. The assembly of Tctex-1 in the dynein complex and its function are largely unknown. Using partially deuterated, $^{15}N$,$^{13}C$-labeled protein samples and transverse relaxation-optimized NMR spectroscopic techniques, the secondary structure and overall topology of Tctex-1 were determined based on the backbone nuclear Overhauser effect pattern and the chemical shift values of the protein. The data showed that Tctex-1 adopts a structure remarkably similar to that of the 8-kDa light chain of the motor complex (DLC8), although the two light chains share no amino acid sequence homology. We further demonstrated that Tctex-1 binds directly to the intermediate chain (DIC) of dynein. The Tctex-1 binding site on DIC was mapped to a 19-residue fragment immediately following the second alternative splicing site of DIC. Titration of Tctex-1 with a peptide derived from DIC, which contains a consensus sequence R/KR/KXXR/K found in various Tctex-1 target proteins, indicated that Tctex-1 binds to its targets in a manner similar to that of DLC8. The experimental results presented in this study suggest that Tctex-1 is likely to be a specific cargo adaptor for the dynein motor complex.**

*Tctex-1* (*t-c*omplex *t*estis-*ex*pressed-1) was originally identified as a multigene family that maps to the *t*-complex, a large region of mouse chromosome 17 (known as *t*-haplotypes) containing four nonoverlapping inversions that suppress recombination (1). Male +/*t*-heterozygotes transmit the mutant chromosome at >99% frequency to their progeny, a non-Mendelian phenomenon known as transmission ratio distortion, and male *t*/*t*-homozygotes are completely sterile. The aberrant expression of *Tctex-1* in the *t*-haplotype mice (4-fold overexpressed in +/*t* and 8-fold in *t*/*t*) was suggested to be functionally related to sterility and transmission ratio distortion (1). This Tctex-1-related meiotic drive hypothesis was supported by the finding that Tctex-1 is a light chain of cytoplasmic as well as flagellar inner arm dynein complexes (2, 3).

Cytoplasmic dynein is a microtubule-based molecular motor involved in various intracelluar motile events including retrograde vesicle transport, axonal transport, mitotic spindle positioning, and nuclear migration (4–7). The dynein motor is a multicomponent protein and contains two heavy chains (~530 kDa), two intermediate chains (DIC[1]; ~74 kDa), four light intermediate chains (~50–60 kDa), and several light chains (DLC; 8, 14, and 22 kDa) (4). Dynein heavy chains directly attach the dynein complex to microtubules and contain ATPase activity, which is required for force generation of the motor. DIC is involved in linking the motor to vesicle-based cargoes by mediating the interaction between dynein and dynactin (8–10). The functions of other dynein subunits are largely unknown because of the complexity of the motor complex.

In addition to functioning as a stoichiometric subunit of the cytoplasmic dynein complex (2, 11), Tctex-1 was also found to interact with a number of cellular proteins of diverse function. Tctex-1 interacts with the N-terminal region of Doc2, and the interaction between these two proteins was suggested to be involved in the dynein-mediated vesicle transport (12). Tctex-1 was also shown to interact with a 19-residue fragment located at the extreme N terminus of $p59^{fyn}$ Src family tyrosine protein kinase (13). Colocalization of Tctex-1 and Fyn at the cleavage furrow and mitotic spindles in T cell hybridomas undergoing cytokinesis points to possible roles of dynein in cell cycle control. Interaction of a lymphocyte surface glycoprotein CD5 with Tctex-1 was suggested to be linked to internalization of CD5 (14). Additionally, Tctex-1 was recently reported to interact directly with the cytoplasmic tail of rhodopsin. This interaction was suggested to be responsible for the transport of rhodopsin-laden vesicles across the inner segment to the base of the connecting cilium (15). The discovery of a large number of functionally unrelated Tctex-1-binding proteins suggests that Tctex-1 is likely to function as an adaptor serving to link specific cargoes to the dynein motor. Because of limited biochemical and structural characterization of Tctex-1, the molecular mechanisms governing the interactions between the protein and its binding partners are unknown.

In this work, we performed a detailed structural characterization of Tctex-1 by NMR spectroscopic techniques. Using purified recombinant proteins, we showed that Tctex-1 binds directly to the intermediate chain of cytoplasmic dynein, and the Tctex-1 binding site was mapped to a short stretch of amino acid residues in the N-terminal region of DIC. We further demonstrate that Tctex-1 shares remarkable structural and target binding similarities with DLC8, although the two light chains share no amino acid sequence homology.

* This work was supported by Grants HKUST6084/98M, 6198/99M, and 6207/00M from the Research Grants Council of Hong Kong and the Human Frontier Science Program (to M. Z.). The NMR spectrometer used in this work was purchased using funds donated to the Biotechnology Research Institute of HKUST by the Hong Kong Jockey Club. The costs of publication of this article were defrayed in part by the payment of page charges. This article must therefore be hereby marked "*advertisement*" in accordance with 18 U.S.C. Section 1734 solely to indicate this fact.

‡ To whom correspondence should be addressed. Tel.: 852-2358-8709; Fax: 852-2358-1552; E-mail: mzhang@ust.hk.

[1] The abbreviations used are: DIC(s), dynein intermediate chain(s); DLC, dynein light chain; GST, glutathione *S*-transferase; NOESY, nuclear Overhauser effect spectroscopy; HSQC, heteronuclear single quantum correlation; TROSY, transverse relaxation-optimized NMR spectroscopy.

## MATERIALS AND METHODS

*Construction of Bacterial Expression Plasmids*—The cDNA encoding mouse Tctex-1 was generously provided by Prof. Yoshimi Takai. The Tctex-1 expression plasmid was constructed by inserting polymerase chain reaction-amplified Tctex-1 gene fragment into the *Nde*I and *Bam*HI sites of the pET3a vector (Novagen).

The full-length mouse DIC gene was constructed by assembling three overlapping genomic clones as described in our earlier work (31). The N-terminal region of DIC (amino acids 1–213) was inserted into the *Bam*HI and *Eco*RI sites of the pGEX-4T-1 vector (Amersham Pharmacia Biotech) for expression of a GST fusion protein. Various truncation, deletion, and point mutations of this DIC fragment were constructed using standard polymerase chain reaction and cloning techniques. The C-terminal WD repeats (amino acids 214–628) were constructed as an N-terminal His-tagged protein (31).

*Protein Expression and Purification*—Tctex-1 was expressed by transforming the pET3a vector containing the Tctex-1 gene into *Escherichia coli* BL21(DE3) host cells. A single colony of *E. coli* cells harboring the expression plasmid was inoculated into 50 ml of LB with 100 $\mu$g/ml ampicillin (LBA). The cell culture was incubated overnight at 37 °C and then inoculated into 1 liter of fresh LBA medium. Tctex-1 expression was induced by the addition of isopropyl-1-thio-$\beta$-D-galactopyranoside when the $A_{600}$ of the culture reached ~0.6. Pelleted cells from 2 liters of culture were resuspended in 50 ml of buffer A (50 mM Tris-HCl, pH 7.9, 5 mM $\beta$-mercaptoethanol, and 1 mM EDTA) containing 0.1 mM phenylmethylsulfonyl fluoride and lysed by sonication. The lysate was centrifuged at 18,000 rpm (Sorvall SS34 rotor) for 30 min at 4 °C, and the supernatant was loaded onto a 50-ml DEAE-Sepharose Fast Flow column (Amersham Pharmacia Biotech). The column was washed with buffer A until the $A_{280}$ reading was steady, and the column was then eluted with 200 ml of buffer A with a linear NaCl gradient of 0–0.3 M. Fractions containing Tctex-1 were pooled and concentrated to about 8 ml before loading onto a Sephacryl-100 (Amersham Pharmacia Biotech) gel filtration column preequilibrated with buffer A containing 0.5 M NaCl. The eluted fractions containing Tctex-1 were pooled and dialyzed against buffer A before loading onto a Mono Q HR 10/10 column (Amersham Pharmacia Biotech). The Mono Q column was washed with buffer A, and Tctex-1 was eluted using 70 ml of the same buffer with an NaCl gradient of 0–0.35 M. The purified Tctex-1 was dialyzed against buffer A and stored at −80 °C.

Various forms of GST-fused DIC mutant proteins were expressed in *E. coli* cells. In a typical purification procedure, cell pellet from 1 liter of culture was resuspended in 25 ml of PBS buffer (140 mM NaCl, 2.7 mM KCl, 10 mM $Na_2HPO_4$, and 1.8 mM $KH_2PO_4$) containing 0.1 mM phenylmethylsulfonyl fluoride. The GST fusion proteins were purified following the instructions of the manufacturer (Amersham Pharmacia Biotech). The purified proteins were dialyzed extensively against PBS prior to binding experiments.

*NMR Sample Preparation*—All NMR samples were prepared by concentrating purified Tctex-1 using a Centriprep-3 (Amicon) ultrafiltration device. The protein was exchanged into the desired NMR sample buffer (50 mM Tris-$d_{11}$, pH 7.0, 2 mM dithiothreitol-$d_{10}$, and 10% $D_2O$), with or without 0.4 M KCl, using ultrafiltration. Preparation of the partially deuterated Tctex-1 followed a protocol described previously with slight modifications (16). Briefly, a single colony of *E. coli* cells harboring the Tctex-1 expression plasmid was inoculated into 50 ml of LBA and incubated overnight at 37 °C. About 4 ml of this overnight culture was inoculated into 200 ml of $^{15}N/H_2O/[^{13}C]$glucose (for $^{2}H,^{15}N,^{13}C$ triple labeling) or $^{15}N/H_2O/[^{12}C]$glucose (for $^{2}H,^{15}N$ double labeling) M9 medium with an initial $A_{600}$ value of ~0.04. The cells were incubated at 37 °C until the $A_{600}$ value reached ~0.5. The cells were spun down at 4 °C and then gently resuspended into 200 ml of $^{15}N$, 80% $D_2O$, $[^{13}C]$glucose or $^{15}N$, 80% $D_2O$, $[^{12}C]$glucose M9 medium. The suspension was diluted five times into 800 ml of $^{15}N$, 80% $D_2O$, $[^{13}C]$glucose or $^{15}N$, 80% $D_2O$, $[^{12}C]$glucose M9 medium to give an $A_{600}$ value of ~0.1. The cultures were incubated at 37 °C until the $A_{600}$ reading reached ~0.5, and Tctex-1 expression was induced by the addition of isopropyl-1-thio-$\beta$-D-galactopyranoside to a final concentration of 0.5 mM. The bacterial culture was incubated overnight at 16 °C before the cells were harvested.

*NMR Spectroscopy*—All NMR experiments were performed on a four-channel Varian Inova 750-MHz spectrometer equipped with a *z*-axis pulsed field gradient unit and an actively shielded triple resonance probe. Sequential backbone assignment of Tctex-1 was completed using three pairs of TROSY-enhanced triple resonance experiments (17), namely HN(CA)CB and HN(COCA)CB; HNCA and HN(CO)CA; HNCO and HN(CA)CO (18–20) on an $^{15}N,^{13}C$ uniformly, 80% $^{2}H$-partially labeled Tctex-1 sample. An $^{1}H$-$^{15}N$ HSQC-NOESY experiment (21) recorded on an $^{15}N$-labeled Tctex-1 sample with a mixing time of 90 ms was used to confirm the sequential assignment. Backbone HN-HN NOEs were obtained using a $^{1}H$-$^{15}N$ HSQC-NOESY-HSQC experiment (22) recorded on an $^{15}N$-uniformly, 80% $^{2}H$-partially labeled Tctex-1 sample with a mixing time of 150 ms. The protein concentrations of all NMR samples were ~1.0 mM.

*GST "Pull-down" Experiments*—For each pull-down assay, 15 $\mu$l of a 75% slurry of GST-Sepharose 4B was first washed three times with 0.5 ml of PBS for equilibration. About 0.1 mg of the GST fusion proteins (250 $\mu$l) was added, and the suspension was agitated at 4 °C for 1 h. The GST-protein-loaded beads were washed four times with 0.5 ml of PBS to remove any unbound protein. A total of 100 $\mu$l of Tctex-1 (35 $\mu$M) solution was added, and the suspension was agitated at 4 °C for an additional 2 h. The beads were then washed four times with 0.5 ml of PBS to remove any unbound Tctex-1 and subsequently boiled with 20 $\mu$l of 2 × SDS-polyacrylamide gel sample buffer. The intensities of the Tctex-1 bands on the SDS-polyacrylamide gel were used to judge the strength of the interaction between Tctex-1 and various GST-DIC fusion proteins.

Competition between DLC8 and Tctex-1 for DIC binding was examined by adding 100-$\mu$l aliquots of DLC8 solutions of increasing concentration to suspensions of Tctex-1 premixed with GST-DIC-loaded GSH-Sepharose beads (at a 1:1 molar ratio of Tctex-1 to GST-DIC). The mixtures were agitated for an additional 2 h, and the beads were subsequently washed four times with 0.5 ml of PBS. The relative amounts of Tctex-1 and DLC8 pelleted by the GSH-Sepharose beads were used to judge possible competition between Tctex-1 and DLC8 for DIC binding.

## RESULTS

*Secondary Structure and Topology of Tctex-1*—To uncover the molecular basis of Tctex-1's cellular function, we characterized the structure of the protein in solution by NMR spectroscopic techniques. An efficient Tctex-1 production and purification procedure was developed, and large quantities of various forms of stable isotope-labeled Tctex-1 were obtained for NMR structural studies. The $^{1}H$-$^{15}N$ HSQC spectrum of $^{15}N$-labeled Tctex-1 showed that the majority of the backbone resonances of the protein were extraordinary broad at various protein concentrations tested (0.1–1 mM). The severe line broadening is likely to be a combined effect of slow to intermediate time scale conformational exchange and nonspecific protein aggregation (for more detail, see below). An array of triple resonance experiments on $^{15}N,^{13}C$-labeled Tctex-1, aiming to obtain the backbone assignment of the protein, failed. Both $^{15}N$- and $^{13}C$-separated three-dimensional NOESY experiments of Tctex-1 showed unusually low amounts of NOE cross-peaks. To circumvent sample aggregation and conformational exchange-induced T2 shortening, partial deuteration (23, 24) of the protein (~80%) together with TROSY techniques (17) were used for NMR characterization of Tctex-1 in solution. Using a combination of TROSY-based HNCA, HN(CO)CA, HN(CA)CB, and HN(COCA)CB triple resonance experiments on a $^{2}H,^{13}C,^{15}N$-triple labeled Tctex-1 sample, we were able to obtain essentially complete backbone resonance assignment of the protein. A $^{15}N$-separated three-dimensional NOESY experiment recorded on a $^{15}N$-labeled Tctex-1, and an HSQC-NOESY-HSQC experiment recorded on a $^{2}H,^{15}N$-labeled protein sample were used to confirm the assignment obtained by the triple resonance experiments. Fig. 1*A* shows the TROSY-HSQC spectrum of Tctex-1 with each backbone amide resonance labeled with amino acid residue name and number. The completion of the backbone chemical shift assignment allowed us to determine the secondary structure of Tctex-1 using a slightly modified chemical shift index approach (25). As both $^{13}C\alpha$ and $^{13}C\beta$ shifts are sensitive to secondary structure, and as they shift to opposite fields in a given secondary structure, a combined $^{13}C\alpha/^{13}C\beta$ secondary shift presented by subtracting the $^{13}C\beta$ secondary shift of a residue from its $^{13}C\alpha$ secondary shift enhances secondary structure-induced chemical shift

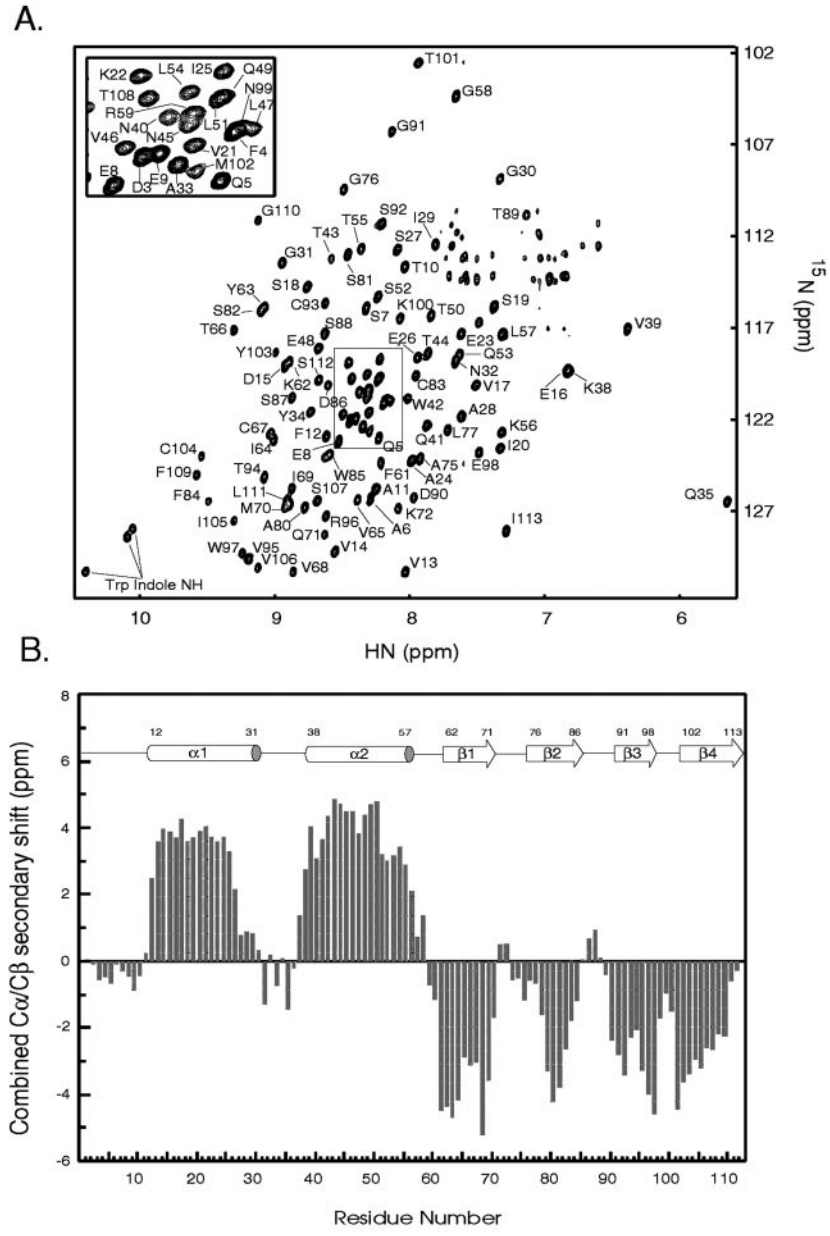


FIG. 1. **Sequential assignment and the secondary structure of Tctex-1.** *Panel A*, $^{1}$H,$^{15}$N-TORSY-HSQC spectrum of $^{15}$N-, 80% $^{2}$H-labeled Tctex-1 in 50 mM Tris-$d_{11}$, pH 7.0, 2 mM dithiothreitol-$d_{10}$, 0.4 M KCl at 22 °C. The assignment of each backbone amide resonance is labeled with the amino acid residue name and number. The crowded region of the spectrum (the *boxed* region at the *center*) is magnified and shown as an *inset* at the *upper left corner* of the spectrum. *Panel B*, combined $^{13}$C$\alpha$/$^{13}$C$\beta$ chemical shift index plot of Tctex-1. In this plot, the secondary chemical shift of each amino acid residue is expressed as the $^{13}$C$\alpha$ secondary shift minus the $^{13}$C$\beta$ secondary shift with a smoothing factor of 3. The secondary structure of Tctex-1 is shown at the *top* of the graph. Amino acid residues 4–7 may adopt a $\beta$-strand-like structure based on relatively small deviation of the combined secondary chemical shifts in this region.

changes of the protein (Fig. 1*B*). Presentation of the secondary structure chemical shifts using combined $^{13}$C$\alpha$/$^{13}$C$\beta$ shifts has the additional advantage of canceling potential secondary shift errors resulted from chemical shift referencing. Based on the data in Fig. 1*B*, we conclude that Tctex-1 is composed of two long N-terminal $\alpha$-helices ($\alpha$1 and $\alpha$2, with starting and ending residues labeled in Fig. 1*B*) followed by four $\beta$-strands ($\beta$1 to $\beta$4). The secondary structure of Tctex-1 derived from the chemical shift data was supported by the backbone NOE patterns of the protein derived from the two three-dimensional $^{15}$N-NOESY experiments (HSQC-NOESY-HSQC and $^{15}$N-separate NOESY, data not shown). The chemical shift values of the residues (Asp-3 to Thr-10) N-terminal to $\alpha$1 indicate that this fragment of Tctex-1 appears to assume a random coil-like structure. The random coil structure of the N-terminal fragment inferred from chemical shift data is also supported by the exceptionally narrow line widths of these residues and the lack of detectable long range backbone NOE of the region. The secondary structure of Tctex-1 shown in Fig. 1*B* is remarkably similar to that of another dynein light chain, DLC8 (26, 27), although the two light chains have very limited amino acid sequence homology.

Next, we determined the overall topology of Tctex-1. To obtain maximal backbone amide resolution, we used an HSQC-NOESY-HSQC experiment recorded on $^{2}$H,$^{15}$N-labeled Tctex-1 to detect backbone HN-HN NOEs. Large numbers of long range, inter-$\beta$-strand NOEs were used to determine the folding topology of the Tctex-1 $\beta$-strands (Fig. 2). The four $\beta$-strands of Tctex-1 form an antiparallel $\beta$-sheet structure with a $\beta$3-$\beta$4-$\beta$1-$\beta$2 arrangement (Fig. 2). Several unambiguous inter-$\alpha$-helical HN-HN NOEs spanning the entire helices (*e.g.* backbone amide NOEs between Asp-15 and Thr-55, Ile-20 and Thr-50, and Gly-30 and Val-39) indicate that the two $\alpha$-helices of Tctex-1 are antiparallel to each other. The detection of long range backbone amide NOEs between amino acid residues from the $\alpha$-helices and $\beta$-strands (*e.g.* NOEs between Ala-28 and Cys-104, Asn-32 and Trp-97, Asn-45 and Cys-67, and Leu-54 and Asp-86) indicate that the two helices pack against the antiparallel $\beta$-sheet of the protein (see Fig. 6, *inset*). The overall topology of Tctex-1 is again very similar to that of DLC8 (26, 27).

*Tctex-1 Binds to a Small Peptide Fragment at the N-terminal*

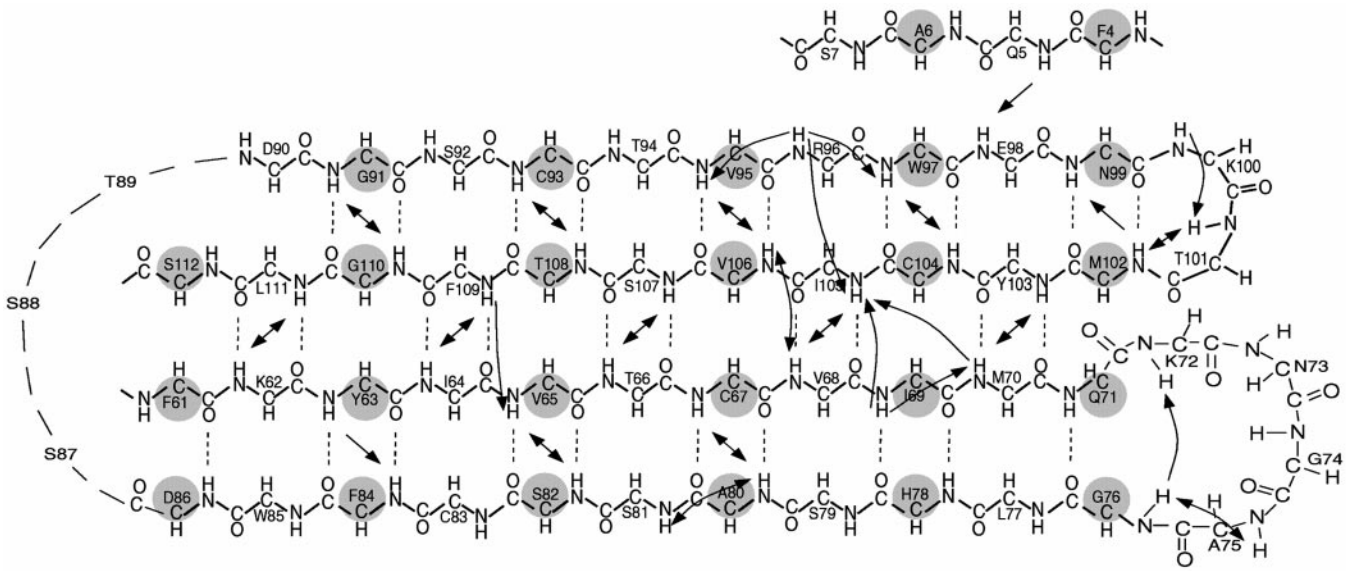


FIG. 2. **The topology of the β-sheet of Tctex-1.** The long range, inter-β-strand HN-HN NOEs (shown with *black arrows*) were used to determine the topology of the four β-strands of Tctex-1. The *dotted lines* are used to indicate expected inter-β-strand hydrogen bonds. The side chains of amino acid residues highlighted with *shaded circles* are on the same side (relative to the β-sheet plane) as the two α-helices of the protein.

*End of DIC*—Earlier biochemical experiments showed that Tctex-1 and DIC cofractionated from a KI-treated cytoplasmic dynein complex preparation, suggesting that Tctex-1 and DIC might interact directly with each other (2, 11). We used purified recombinant proteins to test direct interaction between Tctex-1 and DIC. A GST-fused fragment spanning residues 1–213 of DIC was found to interact robustly with Tctex-1 in the GSH-Sepharose pull-down assay (Fig. 3*B*, *lane 3*), indicating that Tctex-1 and DIC can indeed interact with each other directly. As expected, purified, recombinant full-length DIC was also able bind to Tctex-1 (data not shown). In contrast, the C-terminal part of DIC which contains the highly conserved Trp-Asp repeats failed to bind to Tctex-1 (data not shown). We then mapped the exact Tctex-1 binding site of DIC by creating a series of DIC truncation mutations (Fig. 3*A*). A 19-residue fragment (residues 124–142) of DIC was identified as sufficient for binding to Tctex-1 (for the amino acid sequence of the peptide fragment, see Fig. 3*A*).

Given the overall structural similarities between Tctex-1 and DLC8, we suspected that Tctex-1 might also bind to a short peptide fragment, as does DLC8 (27). To localize the precise Tctex-1 binding site further, we deleted a positive charged, 5-residue fragment (RRLHK) located at the N-terminal end of the 19-residue Tctex-1 binding fragment of DIC (Fig. 4). Deletion of the 5-residue fragment completely abolished the interaction between DIC and Tctex-1, indicating that this 5-residue cassette plays an important role in supporting the Tctex-1·DIC complex formation. However, this 5-residue fragment alone is not sufficient for effective binding to Tctex-1 because a GST fusion peptide containing this 5-residue fragment plus a few amino acid residues at both ends was not able to pull down Tctex-1 (Fig. 4*B*, *lane 5*). These data indicate that both the N- and C-terminal parts of the 19-residue DIC fragment are required for the Tctex-1·DIC complex formation.

*DIC Binds to the β2-Strand and the β2/β3-Loop of Tctex-1*—We next set out to identify the DIC binding region in Tctex-1. To simplify the experiment, we used a synthetic peptide corresponding to the full-length Tctex-1 binding domain of DIC to titrate with partially deuterated $^{15}$N-labeled Tctex-1. Unfortunately, the $^{1}$H-$^{15}$N HSQC of Tctex-1 in the presence of this peptide became exceedingly broad and beyond interpretation, suggesting a severe aggregation of the protein-peptide

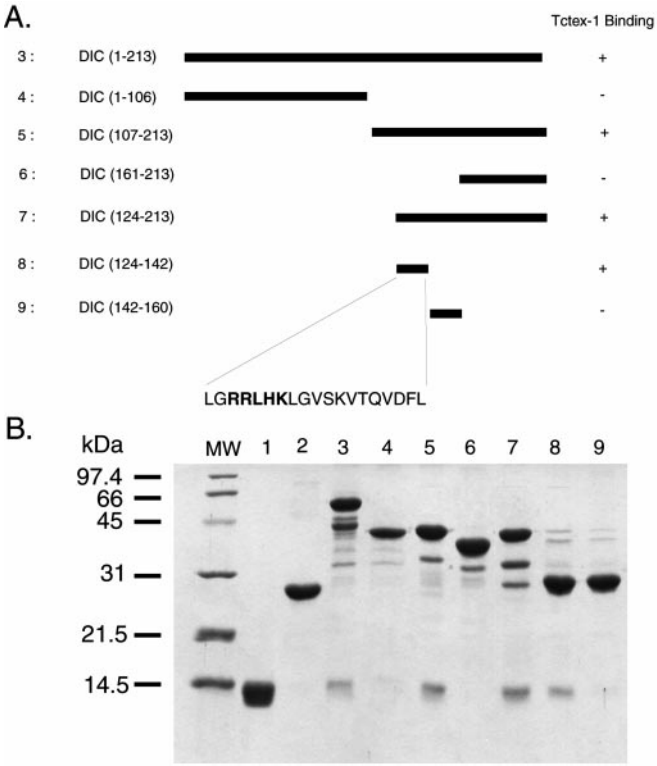


FIG. 3. **Mapping of the Tctex-1 binding domain of DIC.** *Panel A*, schematic diagram showing the various truncation mutants of GST-fused DIC used to map the Tctex-1 binding domain. The binding of each mutant with Tctex-1 is also summarized in the figure. *Panel B*, Coomassie Blue staining of an SDS-polyacrylamide gel showing the interaction between various purified DIC fragments and Tctex-1. The *lane number* in *panel B* corresponds to the *construct number* in *panel A*. Purified Tctex-1 (*lane 1*) was used as a protein marker, and pure GST (*lane 2*) was a negative control.

complex (data not shown). Inspection of the amino acid sequences of a number of Tctex-1 binding regions in various targets revealed a short stretch of consensus sequence of R/KR/KXXR/K (Fig. 5). Although an 11-residue DIC peptide containing the consensus sequence fused to GST was not able to pull down Tctex-1 (the assay requires high affinity binding between

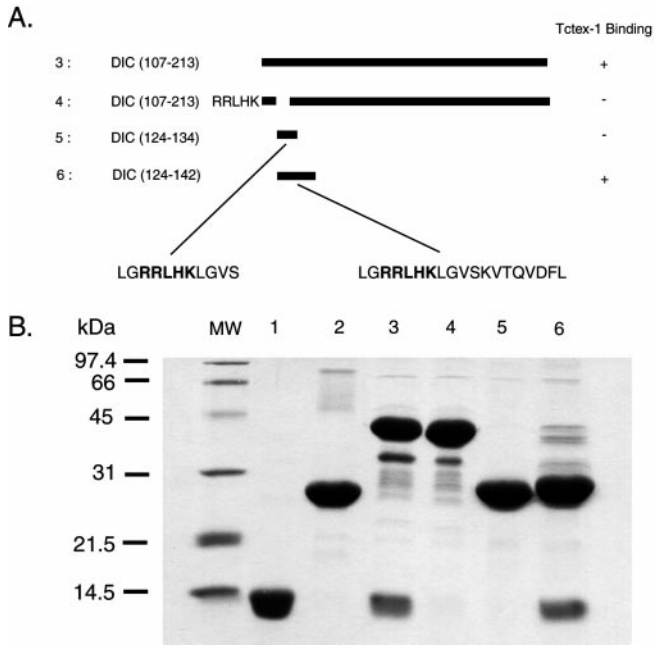


FIG. 4. **Dissection of the Tctex-1 binding domain of DIC.** *A*, schematic diagram showing the truncation and deletion mutants of GST-DIC used to analyze the interaction between Tctex-1 and DIC. The amino acid sequence of *constructs 5* and *6* are shown in the figure. The consensus RRLHR sequence is highlighted with *boldface letters*. *Panel B*, Coomassie Blue staining of an SDS-polyacrylamide gel showing the interaction between Tctex-1 and various GST-DIC fusion proteins. The *lane number* in *panel B* corresponds to the *construct number* in *panel A*. Purified Tctex-1 (*lane 1*) was used as a protein marker, and pure GST (*lane 2*) was a negative control.

| | |
|---|---|
| DIC | -$^{120}$SDSELG**RR**LH**K**LGVSKVTQVDFL$^{142}$- |
| DOC2α | -----$^{1}$MRG**RR**GD**R**MTINIQEHMAIN$^{20}$- |
| DOC2β | ----$^{1}$MTLR**RR**GE**K**ATISIQEHMAID$^{21}$- |
| CD5 cyt | ----$^{379}$LVY**KK**LV**K**KFRQKKQRQWIGPT$^{400}$- |
| Peropsin | ---$^{295}$VAAH**KK**FR**K**AMLAMFKCQPHLA$^{316}$- |
| Fyn | $^{1}$MGCVQCKDKEAAKLTEERD$^{19}$--- |
| Rhodopsin | -$^{328}$LGDDEASATVSKTETSQVAPA$^{348}$- |

FIG. 5. **Sequence alignment analysis of selected Tctex-1 binding domains.** Amino acid sequence alignment of the Tctex-1 binding domains of DIC (this work), DOC2α and DOC2β (12), CD5 antigen (14), and peropsin reveals a consensus R/KR/K*XX*R/K motif in Tctex-1 binding domains (shown in *boldface letters*). However, no obvious consensus sequence can be observed in the Tctex-1 binding domain of p59$^{fyn}$ (13) and rhodopsin (15).

the two proteins; Fig. 3), we anticipated that NMR titration of Tctex-1 with the same 11-residue peptide would allow us to detect the possible interaction between the protein and peptide (even if the interaction were relatively weak). To test this possibility, we titrated $^{15}$N-labeled Tctex-1 with the 11-residue synthetic peptide (LGRRLHKLGVS from residue 124 to 134 of DIC, Fig. 4). Significant chemical shift changes of a number of backbone amide cross-peaks of Tctex-1 were observed during the titration, indicating that the 11-residue DIC peptide can indeed bind to the protein. Fig. 6 shows an overlay plot of the HSQC spectra of Tctex-1 at the start (*blue*) and end (*red*) points of the titration. The amino acid residues that display significant chemical shift changes are labeled, and these amino acid residues are likely to be those involved in the peptide binding. The *inset* of Fig. 6 shows the distribution of the amino acids that undergo significant peptide-induced chemical shift changes, and these residues are found mainly at the end of β2 (Cys-83, Phe-84, Trp-85, and Asp-86) and the β2/β3-loop (Thr-89, Asp-90, and Gly-91) of Tetex-1. In addition, several residues that are in close proximity to this region (*e.g.* Thr-55 and Lys-56 at the end of α1, and Phe-61 and Lys-62 at the start of β1) also experience some chemical shift changes. Based on the data in Fig. 6, we conclude that the β2-strand and the β2/β3-loop are the main DIC binding region in Tctex-1.

*Mutational Analysis of the Consensus Tctex-1 Binding Sequence*—To assess the potential roles of the conserved amino acids in the consensus R/KR/K*XX*R/K sequence of DIC in Tctex-1 binding, we performed a systematic mutational analysis. The data indicate that no single residue in the consensus sequence (RRLHK) plays a dominant role in supporting the Tctex-1·DIC complex formation (Fig. 7). The second arginine residue in the consensus sequence appears to make a slightly larger contribution to the complex formation (Fig. 7*B*, *lane 5*). However, deletion of the whole consensus sequence resulted in complete disruption of the Tctex-1·DIC complex (Fig. 4), suggesting that these amino acid residues may function additively in binding to Tctex-1.

The DIC truncation experiment showed that residues C-terminal to the consensus RRLHK sequence (*i.e.* LGVSKVTQVDFL) are also involved in Tctext-1 binding (Fig. 4). Consistent with this, mutation of Leu-131 to Asn greatly diminished the interaction between Tctex-1 and DIC (Fig. 8, *lane 9*). However, a combination of the consensus RRLHK sequence and Leu-131 is not sufficient for strong binding because the GST-fused peptide containing both the consensus sequence and Leu-131 was not able to form a stable complex with Tctex-1 (Fig. 5, *lane 5*). Further mutational analysis will be required to identify the structural features that are essential for Tctex-1 binding.

*The Tctex-1 and DLC8 Binding Sites in DIC Are Mutually Independent*—The Tctex-1 binding site (residues 124–142, LGRRLHKLGVSKVTQVDFL) identified in this study and the DLC8 binding site (151–155, KETQT) in DIC are immediately next to each other in the amino acid sequence of DIC (Fig. 9, and Ref. 31). Additionally, the Tctex-1 binding site contains a KVTQV sequence that is similar to the KETQT DLC8 binding motif (31). Therefore, there is a possibility that the binding of Tctex-1 and DLC8 on DIC are mutually exclusive. To test this possibility, we performed a binding competition experiment as shown in Fig. 8. In this experiment, equal molar amounts of GST-DIC and Tctex-1 were mixed with increasing molar ratio amounts of DLC8 (Fig. 8). The GST-DIC·Tctex-1·DLC8 ternary complex was pelleted by GSH-Sepharose beads and subsequently analyzed by SDS-polyacrylamide gel electrophoresis. Data in Fig. 8 clearly demonstrate that excess DLC8 does not displace Tctex-1 from DIC, indicating that Tctex-1 and DLC8 can bind simultaneously to DIC. In a reverse experiment, we found that excess Tctex-1 does not compete with DLC8 for binding to DIC, consistent with our conclusion that the Tctex-1 binding site and the DLC8 binding site on DIC are mutually independent (data not shown).

## DISCUSSION

As a part of our continuing effort to understand the structure and function of cytoplasmic DLCs, we performed a detailed structural analysis of Tctex-1 in this study. Using multidimensional TROSY-enhanced NMR spectroscopic techniques, we determined the secondary structure and the topology of Tctex-1 in solution. Tctex-1 shares a remarkably similar structure with DLC8 both at the secondary structure and folding topology levels (26, 27), although the two proteins display very limited amino acid sequence homology. Analogous to DLC8, both gel filtration and chemical cross-linking studies showed that Tctex-1 can exist as a dimer in solution (data not shown). A full structural determination of Tctex-1 and/or its complex with a target peptide is required to answer how the Tctex-1 dimer is assembled in solution. Detailed comparisons of the

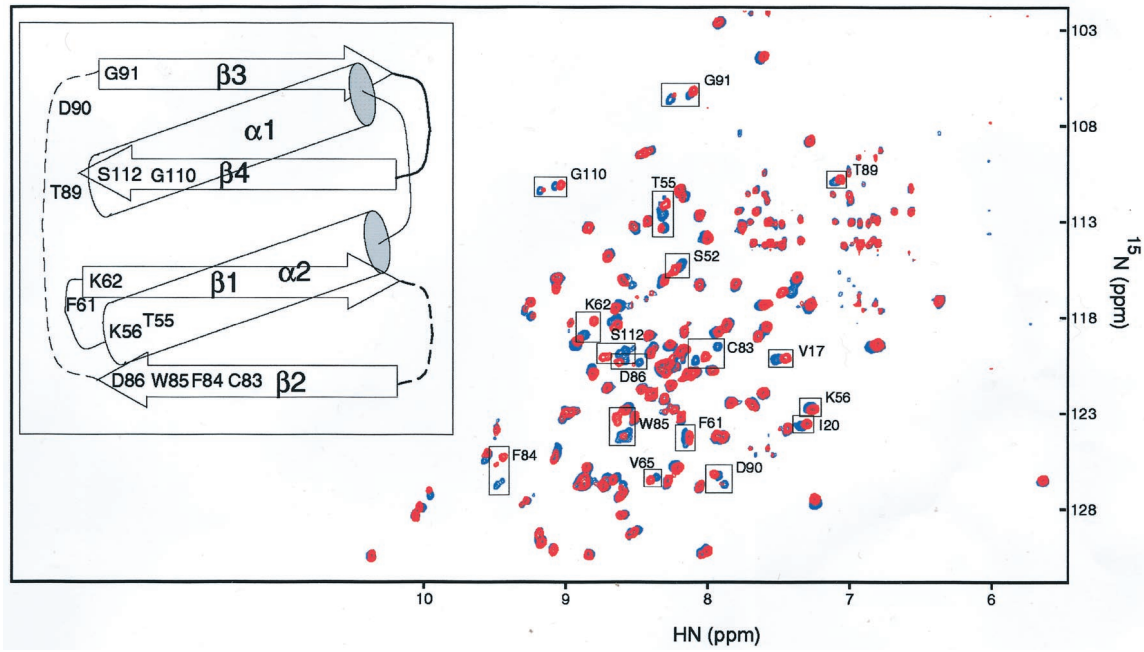


FIG. 6. **Interaction of Tctex-1 with a DIC peptide.** The figure shows an overlay plot of TROSY-HSQC spectra of Tctex-1 at the starting (*blue*) and end (*red*) points of titration with an 11-residue peptide (LGRRLHKLGVS) corresponding to the N-terminal part of the Tctex-1 binding domain of DIC. The concentration of Tctex-1 ($^{15}$N-, 80% $^{2}$H-labeled) is 0.4 mM, and the protein was dissolved in 50 mM Tris-$d_{11}$, pH 7.0, 2 mM dithiothreitol-$d_{10}$. The molar ratio of the DIC peptide to Tctex-1 at the final point of the titration is 2:1. The residues that show significant chemical shift changes upon the addition of the DIC peptide are marked with *open boxes*, and these amino acid residues are mapped to the topology structure of Tctex-1 shown as an *inset* in the figure. The *dashed lines* in the topology diagram of Tctex-1 are used to indicate the uncertainty of the connections of the β-strands due to potential domain swapping of the Tctex-1 dimer.

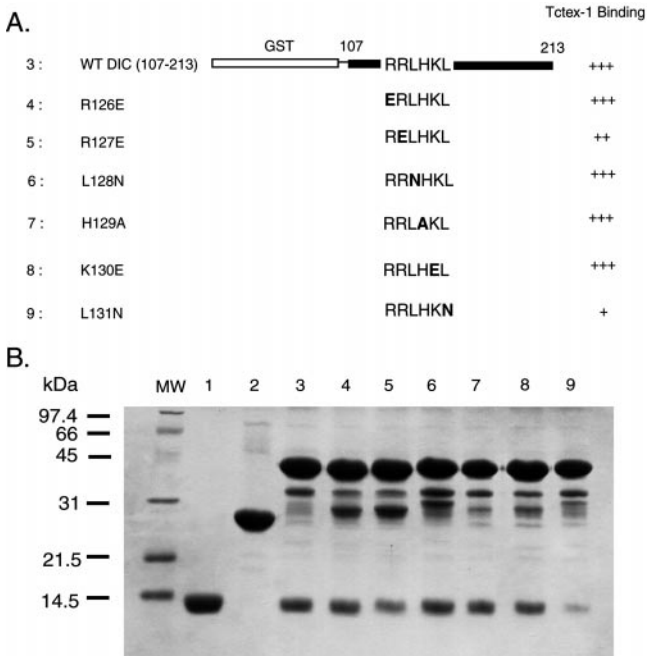


FIG. 7. **Mutational analysis of the consensus Tctex-1 binding motif.** *Panel A*, schematic diagram showing the individual mutations of the DIC fragment created in the experiment. The binding of each mutant with Tctex-1 is also summarized in the figure. *WT*, wild type. *Panel B*, Coomassie Blue staining of an SDS-polyacrylamide gel showing the interaction between various DIC mutants and Tctex-1. The *lane number* in *panel B* corresponds to the *construct number* in *panel A*. Purified Tctex-1 (*lane 1*) was used as a protein marker, and pure GST (*lane 2*) was a negative control.

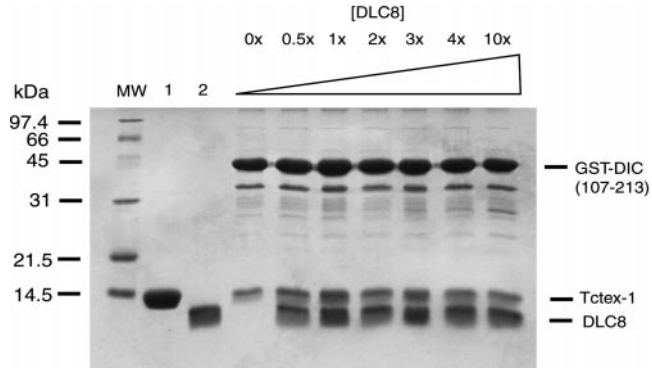


FIG. 8. **Tctex-1 and DLC8 can simultaneously bind to DIC.** Coomassie Blue staining of an SDS-polyacrylamide gel showing that excess DLC8 does not compete with Tctex-1 for binding to DIC. *Lanes 3–9* show Tctex-1 and DLC8 pulled down by GST-DIC. The molar ratios of DLC8 (relative to Tctex-1 and GST-DIC, which were premixed at an equal molar ratio) used in the dose-dependent competition experiment are indicated at the *top* of each *lane*. *Lanes 1* and *2* are purified Tctex-1 and DLC8 protein markers.

structures of Tctex-1 and DLC8, both in apo- and target-bound forms, will help to elucidate how the two structurally similar light chains distinguish their respective targets.

In DLC8, target peptides bind to the protein by augmenting the β-sheet via the β2-strand in an antiparallel fashion (26, 27). Our NMR studies indicated that Tctex-1 binds a target peptide derived from DIC using a mechanism similar to that of DLC8 (*i.e.* the β2-strand and the β2/β3-loop are the major target binding regions for both proteins) (Fig. 6). It is possible that the short DIC peptide (LGRRLHKLGVS) used in the NMR titration experiment may also bind to Tctex-1 by pairing with the β2-strand of the protein. However, we also notice significant differences between Tctex-1 and DLC8 in their respective target bindings. For example, DLC8 is capable of binding to a KXTQT motif-containing peptide, which is as short as 9 residues, with high affinity and specificity (27, 31). In contrast, the Tctex-1-binding peptide is likely to be significantly longer. An 11-residue DIC peptide containing a consensus R/KR/KXXR/K sequence with a few amino acid residue extensions at both ends

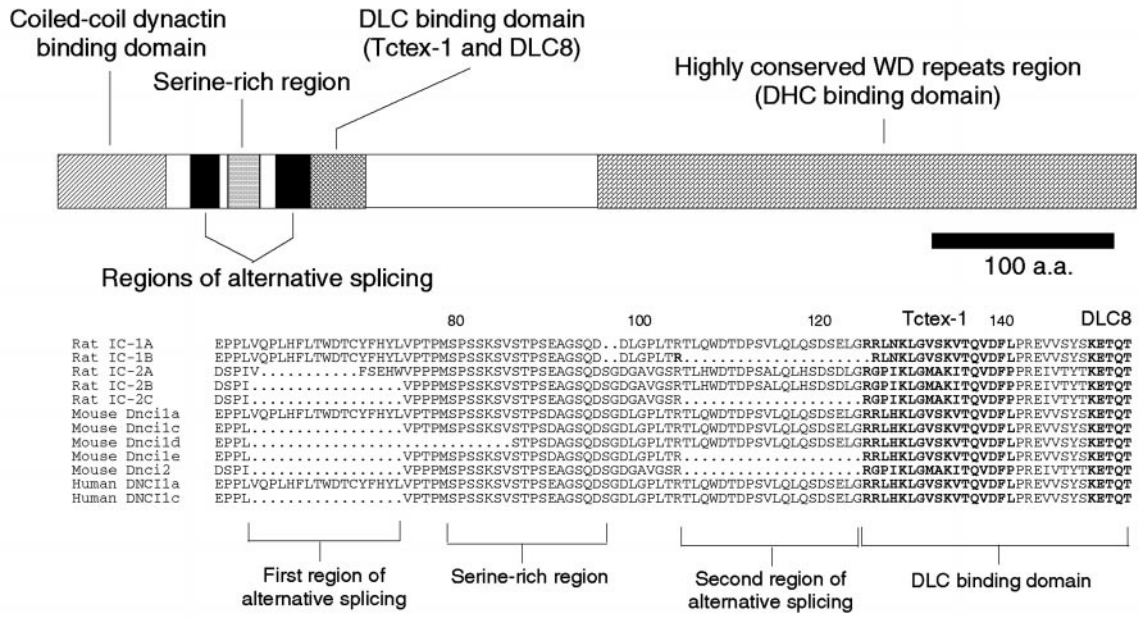


FIG. 9. **Summary of the domain organization of cytoplasmic DIC.** Cytoplasmic DIC contains an N-terminal coiled-coil domain that binds to dynactin complex followed by alternative splicing sites and a highly conserved Ser-rich region sandwiched by the two alternative splicing sites. Immediately following the second alternative splicing site are the nonoverlapping Tctex-1 and DLC8 binding sites. The C-terminal Trp-Asp repeat is expected to form $\beta$-propeller structures, and this domain is likely responsible for binding to the heavy chain of the dynein complex. A partial amino acid sequence alignment of various isoforms of cytoplasmic DIC including the alternative splicing sites, Ser-rich region, and the two light chain binding regions is also included in the figure. The Tctex-1 and DLC8 binding sites of DIC are highlighted with *boldface letters*, and these two regions are highly conserved.

was not able to bind to Tctex-1 with high affinity (Fig. 5). To achieve high affinity binding, an additional ~10 amino acids C-terminal to the RRLHK sequence of DIC are required. Given the length of the Tctex-1-binding peptide, the target binding site on Tctex-1 is likely to involve regions other than the $\beta$2-strand and the $\beta$2/$\beta$3-loop of the protein. Unfortunately, because of the poor behavior of Tctex-1 complexed with a synthetic peptide containing the complete Tctex-1 binding region of DIC in solution, we were not able to determine the exact regions of Tctex-1 which are involved in target binding.

Although the amino acid residues downstream of the consensus R/KR/K*XX*R/K sequence are necessary for effective binding of Tctex-1 and its targets, sequence alignment analysis shows that no obvious homology can be observed in these regions (Fig. 6). The sequence downstream of the consensus R/KR/K*XX*R/K sequence in DIC is a mix of hydrophobic and hydrophilic residues (LGVSKVTQV). The same region in CD5 is composed mainly of hydrophilic residues; only one hydrophobic residue occurs (KFRQKKQRQ). It seems that Tctex-1 is capable of binding to a number of targets with diverse amino acid sequences, a phenomenon that was also observed for DLC8 (27). Mutational analysis indicated that polar/charged interactions between the positively charged consensus sequence R/KR/K*XX*R/K and negatively charged amino acids from Tctex-1 are likely to play important roles in binding specificity because deletion of all three positively charged residues of DIC abolished its binding to Tctex-1. Hydrophobic interactions between amino acid residues downstream of the consensus sequence and Tctex-1 are also expected to provide favorable binding energy for complex formation, as mutation of Leu-131 of DIC to Asn greatly reduced its affinity for Tctex-1 (Fig. 7).

Because of alternative splicing of the two DIC genes, there at least five different isoforms of DIC in mammals (8, 10, 28, 29). Fig. 9 shows a schematic diagram of the domain organization of DIC. The function of the C-terminal Trp-Asp repeats is still unknown. The high amino acid sequence homology of the Trp-Asp repeats domain of DICs from both cytoplasmic and axonemal DICs suggests that this domain is likely to be responsible for attaching DICs to the heavy chains of the motor complex. The N-terminal ~120 residues (including the two alternative splicing sites and the Ser-rich region) of DIC was identified to interact with dynactin. The discovery of the interaction between DIC and dynactin suggested that DIC functions as the adaptor to link the motor complex to its vesicle-based cargoes (8). Following the dynactin binding region of DIC are the Tctex-1 and DLC8 binding regions. Because both light chains are capable of binding a large number of functional unrelated proteins, it is likely that the light chains function as motor adaptors for transporting various specific cargoes. This hypothesis is supported by the observation that the two target binding sites of DLC8 (and also likely Tctex-1) can simultaneously bind to DIC and one of its target proteins.[2] Unlike kinesins and myosins that contain a large number of isoforms, cytoplasmic dynein contains two copies of identical heavy chains with motor activities. It is likely that a combination of various light chains and light intermediate chains as well as intermediate chains allows a single cytoplasmic dynein complex to move a vast number of molecular cargoes along microtubules.

The dynactin binding region of DIC contains alternative splicing sites and potential protein phosphorylation sites within the Ser-rich region (Fig. 9). The dynein light chain binding domains in DIC are situated immediately C-terminal to the second alternative splicing region. This means that neither alternative splicing nor phosphorylation of DIC would have any effect on Tctex-1 and DLC8 binding on DIC. A competition binding assay of Tctex-1 and DLC8 on DIC showed that the bindings of Tctex-1 and DLC8 on DIC are mutually independent (Fig. 8), suggesting that both Tctex-1 and DLC8, together with their unique cargoes, can bind to DIC simultaneously. Cytoplasmic dynein contains another light chain called RP3, which shares 52% amino acid identity to Tctex-1.

[2] K. W.-H. Lo, and M. Zhang, unpublished results.

However, RP3 displays distinct target binding properties when compared with Tctex-1. In contrast to what was observed for Tctex-1, RP3 does not interact with rhodopsin (15) or Doc2 (12). Tctex-1 and RP3 are regulated differentially in both a developmental and tissue-specific manner. Functionally distinct populations of cytoplasmic dynein may contain different Tctex-1 family light chains. Subcellular localization of specific light chains, including Tctex-1, may also contribute to the functional differences of dynein complexes (30). We do not know whether RP3 directly binds to DIC, or if it does, whether Tctex-1 and RP3 bind to DIC in a mutually exclusive manner. Further work is required to address these questions. We further note that although the amino acid sequence of the DLC8 and Tctex-1 binding region shown in Fig. 9 is highly conserved in cytoplasmic DIC, these sequences are not clearly identifiable in axonemal DICs, suggesting a possible difference in the assembly of the light chains between axonemal and cytoplasmic dyneins.

*Acknowledgments*—We thank Prof. Yoshimi Takai for providing the Tctex-1 gene and Dr. Jim Hackett for careful reading of the manuscript.

REFERENCES

1. Lader, E., Ha, H. S., O'Neill, M., Artzt, K., and Bennett, D. (1989) *Cell* **58,** 969–979
2. King, S. M., Dillman, I. I. I., J. F., Benashski, S. E., Lye, R. J., Patel-King, R. S., and Pfister, K. K. (1996) *J. Biol. Chem.* **271,** 32281–32287
3. Harrison, A., Olds-Clarke, P., and King, S. M. (1998) *J. Cell Biol.* **140,** 1137–1147
4. King, S. M. (2000) *Biochim. Biophys. Acta* **1496,** 60–75
5. Karki, S., and Holzbaur, E. L. (1999) *Curr. Opin. Cell Biol.* **11,** 45–53
6. Hirokawa, N. (1998) *Science* **279,** 519–526
7. Vallee, R. B., and Sheetz, M. P. (1996) *Science* **271,** 1539–1544
8. Vaughan, K. T., and Vallee, R. B. (1995) *J. Cell Biol.* **131,** 1507–1516
9. Ma, S., Trivinos-Lagos, L., Graf, R., and Chisholm, R. L. (1999) *J. Cell Biol.* **147,** 1261–1273
10. Susalka, S. J., Hancock, W. O., and Pfister, K. K. (2000) *Biochim. Biophys. Acta* **1496,** 76–88
11. King, S. M., Barbarese, E., Dillman, I. I. I., J. F., Benashski, S. E., Do, K. T., Patel-King, R. S., and Pfister, K. K. (1998) *Biochemistry* **37,** 15033–15041
12. Nagano, F., Orita, S., Sasaki, T., Naito, A., Sakaguchi, G., Maeda, M., Watanabe, T., Kominami, E., Uchiyama, Y., and Takai, Y. (1998) *J. Biol. Chem.* **273,** 30065–30068
13. Campbell, K. S., Cooper, S., Dessing, M., Yates, S., and Buder, A. (1998) *J. Immunol.* **161,** 1728–1737
14. Bauch, A., Campbell, K. S., and Reth, M. (1998) *Eur. J. Immunol.* **28,** 2167–2177
15. Tai, A. W., Chuang, J.-Z., Bode, C., Wolfrum, U., and Sung, C.-H. (1999) *Cell* **97,** 877–887
16. Rosen, M. K., Gardner, K. H., Willis, R. C., Parris, W. E., Pawson, T., and Kay, L. E. (1996) *J. Mol. Biol.* **263,** 627–636
17. Pervushin, K., Braun, D., Fernandez, C., and Wuthrich, K. (2000) *J. Biomol. NMR* **17,** 195–202
18. Kay, L. E., and Gardner, K. H. (1997) *Curr. Opin. Struct. Biol.* **7,** 722–731
19. Kay, L. E. (1997) *Biochem. Cell Biol.* **75,** 1–15
20. Clore, G. M., and Gronenborn, A. M. (1998) *Trends Biotechnol.* **16,** 22–34
21. Zhang, O., Forman-Kay, J. D., Shortle, D., and Kay, L. E. (1997) *J. Biomol. NMR* **9,** 181–200
22. Ikura, M., Bax, A., Clore, G. M., and Gronenborn, A. M. (1990) *J. Am. Chem. Soc.* **112,** 9020–9022
23. Grzesiek, S., Anglister, J., Ren, H., and Bax, A. (1993) *J. Am. Chem. Soc.* **115,** 4369–4370
24. Yamazaki, T., Lee, W., Arrowsmith, C. H., Muhandiram, D. R., and Kay, L. E. (1994) *J. Am. Chem. Soc.* **116,** 11655–11666
25. Wishart, D. S., Sykes, B. D., and Richards, F. M. (1992) *Biochemistry* **31,** 1647–1651
26. Liang, J., Jaffrey, S. R., Guo, W., Snyder, S. H., and Clardy, J. (1999) *Nat. Struct. Biol.* **6,** 735–740
27. Fan, J.-S., Zhang, Q., Tochio, H., Li, M., and Zhang, M. (2001) *J. Mol. Biol.* **306,** 97–108
28. Nurminsky, D. I., Nurminskaya, M. V., Benevolenskaya, E. V., Shevelyov, Y. Y., Hartl, D. L., and Gvozdev, V. A. (1998) *Mol. Cell. Biol.* **18,** 6816–6825
29. Crackower, M. A., Sinasac, D. S., Xia, J., Motoyama, J., Prochazka, M., Rommens, J. M., Scherer, S. W., and Tsui, L. C. (1999) *Genomics* **55,** 257–267
30. Tai, A. W., Chuang, J.-Z., and Sung, C.-H. (1998) *J. Biol. Chem.* **273,** 19639–19649
31. Lo, K. W.-H., Naisbitt, S., Fan, J.-S., Sheng, M., and Zhang, M. (2001) *J. Biol. Chem.* **276,** 14059–14066